Pure & Appl. Chem., Vol. 62, No. 5, pp. 825–838, 1990.
Printed in Great Britain.

A critical review of solid rocket propellant transient flame models

Luigi De Luca

Dipartimento di Energetica, Politecnico di Milano
32 Piazza Leonardo da Vinci, 20133 Milano, Italy

Abstract – A critical review is offered of the commonly implemented flame models for computing transient burning rates and intrinsic combustion stability of solid rocket propellants. After illustrating merits and limitations of each, a new flame model is described, by means of a unified mathematical formalism, incorporating all of the previous knowledge and allowing ground for further extensions. In particular, a better and closer agreement with experimental information is enforced. The general feature of the new model, called $\alpha\beta\gamma$, is the capability to describe spatially thick gas–phase flames, when necessary, allowing pressure and/or temperature dependence of several of the relevant parameters. With proper care and within current limitations, the $\alpha\beta\gamma$ transient flame model is applicable to both double–base and composite solid rocket propellants. However, in order to accomplish further progress more fundamental work in the area of characteristic gas–phase times is required.

NOMENCLATURE

c	= specific heat, cal/g K
C	= c / c_{ref}, nondimensional specific heat
d	= thickness, cm
$\tilde{E}$	= activation energy, cal/mol
$E_{()}$	= $\tilde{E} / \Re / T_{(),ref}$, nondimensional activation energy
Fo	= $Io / \tilde{q}_{ref}$, nondimensional external radiant flux
H	= Q / Q_{ref}, nondimensional heat release
Io	= external radiant flux intensity, cal/cm^2 s
k	= thermal conductivity, cal/cm s K
K	= k / k_{ref}, nondimensional thermal conductivity
M	= maximum value of chemical reaction rate
n	= ballistic exponent
n_s	= pressure exponent in the pyrolysis law
p	= pressure, atm
p_{ref}	= 68 atm, reference pressure
P	= p / p_{ref} , nondimensional pressure
q	= $\tilde{q} / \tilde{q}_{ref}$, nondimensional energy flux
$\tilde{q}$	= energy flux intensity, cal/ cm^2 s
$\tilde{q}_{ref}$	= $\rho_c c_c r_{b,ref} (T_{s,ref} - T_{ref})$, reference energy flux, cal/ cm^2 s
Q	= heat release, cal/g (positive exothermic)
Q_{ref}	= $c_{ref} (T_{s,ref} - T_{ref})$, reference heat release, cal/g
r_b	= burning rate, cm/s
$r_{b,ref}$	= $r_b(p_{ref})$, reference burning rate, cm/s
$\bar{r}_\lambda$	= average optical reflectivity of the burning surface, %
R	= $r_b / r_{b,ref}$, nondimensional burning rate
$\Re$	= universal gas constant; 1.987 cal/mol K or 82.1 atm cm^3/ mol K
t	= time coordinate, s
T	= temperature, K
T_{ref}	= 300 K , reference temperature
$T_{s,ref}$	= $T_s(p_{ref})$, reference surface temperature, K
u	= gas velocity, cm/s
U	= $u / r_{b,ref}$, nondimensional gas velocity

w = power of pyrolysis law
=
W = average molecular mass of gas mixture, g/mol
x = space coordinate, cm
X = $x / (\alpha_{ref} / r_{b,ref})$, nondimensional space coordinate
Z = parameter of elongated flame kinetics

Greek symbols

α = thermal diffusivity, cm^2/s; also: parameter of a transient flame model
β = parameter of a transient flame model
γ = parameter of a transient flame model
ϵ = nondimensional reaction rate
$\bar{\tilde{\epsilon}}_{\lambda}$ = average optical emissivity of the burning surface, %
θ = $(T - T_{ref}) / (T_{s,ref} - T_{ref})$, nondimensional temperature
$\Upsilon_{()}$ = $T_{()} / T_{(),ref}$, nondimensional temperature
ρ = density, g/cm^3
τ = $t / (\alpha_{ref} / r_{b,ref}^2)$, nondimensional time coordinate
$<\tau'>$ = $\tau (C_g / K_g) (\rho_c / <\rho_g>)$, nondimensional characteristic time parameter
φ = $Q_g \rho_g \tilde{\epsilon}_g$, heat release rate per unit volume, $cal/ cm^3 s$

Subscripts and superscripts

c = condensed–phase
dz = dark–zone
f = flame
fz = fizz–zone
g = gas–phase
s = burning surface
c,s = burning surface, condensed–phase side
g,s = burning surface, gas–phase side
ref = reference
λ = spectral
$< >$ = space average
– = steady state
= = average over chemical composition
$-\infty$ = far upstream
~ = dimensional value

Abbreviations

AN = Ammonium Nitrate (NH_4NO_3)
AP = Ammonium Perchlorate (NH_4ClO_4)
DB = Double–Base
GAP = Glycidyl Azide Polymer
HMX = cyclotetramethylene tetranitramine
KTSS = Krier–T'ien–Sirignano–Summerfield
KZ = Kooker–Zinn
LIF = Laser Induced Fluorescence
LC = Levine–Culick
MTS = Merkle–Turk–Summerfield
PNC = Plastisol NitroCellulose
TMETN = TriMethylolEthane TriNitrate

1 BACKGROUND

Within the framework of overall monodimensionality in space, gas–phase quasi–steadiness in time, and thermal nature of combustion model, for several classes of solid rocket propellants transient burning can be numerically simulated and intrinsic combustion stability analytically predicted, reasonably well. The theoretical treatment by this research group is based on fundamental principles only; among its features there is the fact that, over a wide range of operating conditions, the combustion model incorporates and/or attempts to reproduce the most detailed experimental information available. Nevertheless, the models currently available from the competent open literature feature unnecessary restrictions of validity or suffer of erroneous and/or arbitrary assumptions. It is the purpose of this paper to review the field of transient flame modeling for solid rocket propellants, point out limitations, and suggest ways to overcome them. In addition, comments will be provided as to the intrinsic combustion stability properties embedded in any transient flame model.

Two important features have first to be recognized. Double–base (DB) propellants, whether catalyzed or not, clearly manifest a multi–zone flame structure over a large pressure range. However, for most current compositions burning at pressures below, say 150 atm, the dark–zone effectively filters away the heat feedback to the burning surface from the luminous–zone. On the other hand, for most current compositions overall monodimensionality in space requires a minimum operating pressure of, say 2 atm. In addition, the particular but important class of catalyzed DB manifests the peculiar effect of super–rate burning, usually in a narrow range near the low end of the above defined pressure interval, consisting of a spectacular increase of burning rate with ballistic exponent largely bigger than 1. This implies that, within wide pressure limits, modeling of DB flames is conveniently reduced to fizz–zone modeling, except perhaps the narrow pressure range over which super–rate occurs.

Heterogeneous or composite propellants, in particular ammonium perchlorate (AP)–based compositions, manifest a pronounced dependence of their combustion properties on the statistics of the multidisperse oxidizing particle population. Unfortunately, nonlinear transient effects in the gas–phase appear impossible to be accounted for by the present monodimensional theories. This implies that those effects will be considered only roughly, and to the extent in which steady–state combustion properties are experimentally affected by different statistics of the multidisperse oxidizing particle population. For currently available transient flame models, treatment of heterogeneous propellants is inherently ensemble averaged.

It is important to underline that a burning propellant is essentially identified by the following four steady–state dependences:

1. experimental burning rate vs pressure $\bar{r}_b = r_b(\bar{p})$;
2. experimental surface temperature vs pressure $\bar{T}_s = T_s(\bar{p})$;
3. experimental surface heat release vs pressure $\bar{Q}_s = Q_s(\bar{p})$;
4. experimental or computed flame temperature $\bar{T}_f = T_f(\bar{p})$.

Should any of these pieces of information be missing, then appropriate assumptions have to be made, which however transform the problem under scrutiny into an exercise of limited use. It is stressed that experimental knowledge of steady behavior is a prerequisite to solve unsteady problems or predict intrinsic stability. As to the flame temperature, in general results from standard thermochemical codes are adequate as long as the operating pressure is larger enough than the corresponding pressure deflagration limit (PDL).

A review of fundamental contributions in the general area of transient flame modeling is offered in the next section. Specific questions concerning spatial distribution of heat release rate in both gas–phase and condensed–phase are respectively dealt with in the successive two sections (3 and 4). After illustrating merits and limitations of relevant contributions, a unified mathematical formalism based on the flame model being developed by the Milan group is presented (section 5). Differences in terms of both transient burning and intrinsic combustion stability are discussed, by comparing pertinent gas–phase working maps deduced from different flame models. Needs of further improvements are pointed out in the final section.

2 LITERATURE SURVEY

The only paper explicitly devoted to a critical review of transient flame model is rather old (ref. 1, presented in 1969), but nicely complements this work; although some errors were lately corrected by the authors (with particular reference to the Zeldovich–Novozhilov approach pursued in USSR), the meaning of quasi–steady gas–phase in transient burning is vividly illustrated. A very informative review is included in chapter 10 of ref. 2. The current open literature scenario can be portrayed as follows.

Transient flames of AP–based composite propellants were successfully modelled by Summerfield and coworkers (ref. 3) by enforcing a spatially uniform heat release rate distribution in a layer of small thickness (not exactly defined by the authors) attached to the burning surface (anchored flame model). Very similar approaches were followed in refs. 4–5, although different physical pictures were invoked. Both refs. 4 and 5 extended somewhat the applicability of ref. 3, in particular allowing a specific heat ratio $c_c / c_g \neq 1$ between condensed– and gas–phase; see section 4. However, the model of ref. 4 does not necessarily recover the steady–state dependence on pressure, while the model of ref. 5 includes a pressure dependent pyrolysis ($n_s \neq 0$) awkward to implement at least under transient burning.

At any rate, if the relevant equations are properly combined, the heat feedback laws provided by these flame models (refs. 3–5) are identical, as discussed in section 5. The heat release rate distribution is mathematically described by a rectangular pulse (even though several investigators call it a "step function", which is misleading); see Fig. 1a for a schematic sketch. This kind of flame, in the following denoted as KTSS, is physically representative of combustion processes controlled by mass diffusion. Notice that in the original paper (ref. 3) both the full expression and a "linearized" (in the sense $q_{g,s} \approx 1/r_b$) versions of the heat feedback to the burning surface were provided. Nonetheless, most of the successive researchers adopted the same linearized procedure, which inhibits applications of the resulting heat feedback to ignition, extinction, and in general transient combustion processes involving burning rates appreciably lower than the corresponding steady reacting values; this is a common error in literature.

More detailed and systematic calculations (yet without specific applications) of transient flame models and structures were performed by Culick and coworkers (refs. 6–7). In particular, a Dirac delta function was suggested to offer a convenient description of flames with a sharp heat release rate distribution in space (flame sheet model). This flame, schematically represented in Fig. 1b, is obviously of vanishing thickness. Physically, this kind of flame is representative of combustion processes controlled by chemical kinetics with a very large activation energy. The implementation of delta funtions, initially suggested by Culick, was accepted by several investigators; for example, see ref. 8. However, this mathematical approach is in most cases unrealistic; at any rate, it exhibits very little intrinsic combustion stability. Details are given in next sections.

Other investigators resort to involved physical modeling, not deduced from first principles (for example, a recent attempt is reported in ref. 9). This kind of efforts, in spite of its practical applications, is not considered here.

The work of ref. 10 (MTS flame) is of particular interest for the purpose of this paper. The heat release rate distribution in space was modelled by combining a rectangular pulse (KTSS flame) with a delta function (flame sheet) in the first and only attempt, known to this author, to account at the same time for both chemical kinetics and mass diffusion effects in transient flames. In the opinion of this writer, however, the unique contribution by Summerfield and coworkers in ref. 10 is the introduction of the characteristic gas–phase times for both chemical kinetics (for which a second order reaction occurring wholly at the highest flame temperature was assumed) and mass diffusion (for which temperature effects also were taken into account). In all other transient flame models, no characteristic time for the gas–phase processes was explicitly considered. In spite of its conceptual sophistication, the whole MTS approach depends on some arbitrary assumption as to the resulting characteristic time and on the need to select appropriate constants for the two individual characteristic times (kinetic and diffusive). It is suggested (ref. 10) to determine these two constants, for each propellant, by the best fit of the steady state burning rate computed by MTS to the corresponding experimental data. Although often feasible, this is a weakness of MTS flame.

An important objective of transient flame modeling would be to relax the quasi–steady gas–phase assumption, which mandatorily restricts the practical applications of the pertinent models to a frequency range from 0 to some 1000 Hz. Unfortunately, this is not yet ready for a full scientific attack. Nevertheless, some attempts were made in the past. T'ien was the first to emphasize this aspect of the problem in 1972 (ref. 11). Later, Suhas and Bose (ref. 12) combined the unsteady gas–phase continuity equation with a standard KTSS linearized heat feedback law; their treatment is questionable, but the importance of the finite time associated with the gas–phase processes cannot be overlooked.

Further comments about open literature contributions are reported in the following two specialized sections respectively on gas–phase and burning surface heat release submodels.

3 GAS-PHASE HEAT RELEASE

All of the above investigations resort to simple mathematical functions to describe the space distribution of heat release rate. How good is this? A critical review of these "classical" approaches and comments about the state of the art in this area were already offered by the author in 1984 (see pp. 692–702 of ref. 13). Following hints from several investigators (refs. 14–18) , detailed and systematic work carried out by the Milan group (refs. 19–24) clearly indicates that the rate of heat release is neither uniform nor sharp in space, but rather features an elongated structure with heat release rate very intense near the burning surface and gradually weakening in the tail. This comet–lile flame structure is schematically sketched in Fig. 1c. The experiments of ref. 19 were all conducted for a catalyzed DB, in a pressure range spanning from subatmospheric to 38 atm. Similar experimental evidence, apparently available in the Soviet literature since longtime, is broadly discussed by Zenin (refs. 14–15), who remarked that this flame structure is typical of both "powders and gasless systems" (p. 446 of ref. 14). Experimental evidence in the open USA literature is sporadic: similar results were found for a nitrocellulose strand (containing 1% stabilizer) burning at about 28 atm (p. 883 of ref. 16) and for a PNC/TMETN (a noncatalyzed DB, containing particulate nitrocellulose, whose thermal profiles were measured by Kubota in ref. 17) burning at about 1 and 21 atm (p. 63 and p. 64 of ref. 18). In addition, all of the above experimental thermal profiles consistently show a convex temperature distribution, increasing more or less slowly while approaching the maximum value (see sketch in Fig. 1c). Yet, anchored or KTSS type of flame models essentially predict a linear temperature distribution, while flame sheet models predict a concave temperature distribution. Finally, the flame thickness experimentally evaluated from the above thermal profiles generally turns out much larger than the value predicted by anchored flame models. In the case of flame sheet models, the chemically reacting region is of vanishing thickness while the maximum temperature location can in principle be placed anywhere (but usually is placed at a distance from the burning surface even shorter than that predicted by anchored flame models).

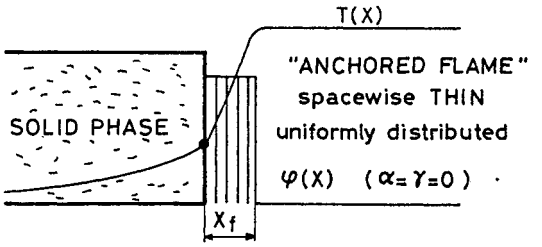

Fig. 1a

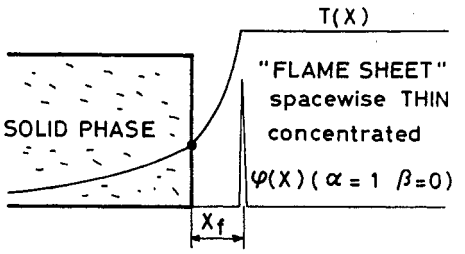

Fig. 1b

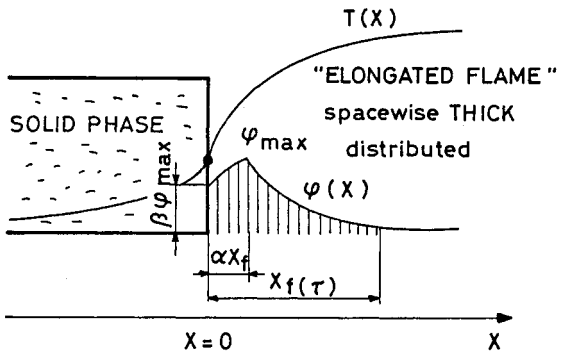

Fig. 1c

Fig. 1. Schematic sketch of heat release rate space distribution according to:
(a) anchored transient flame models;
(b) sheet transient flame models;
(c) αβγ transient flame models.

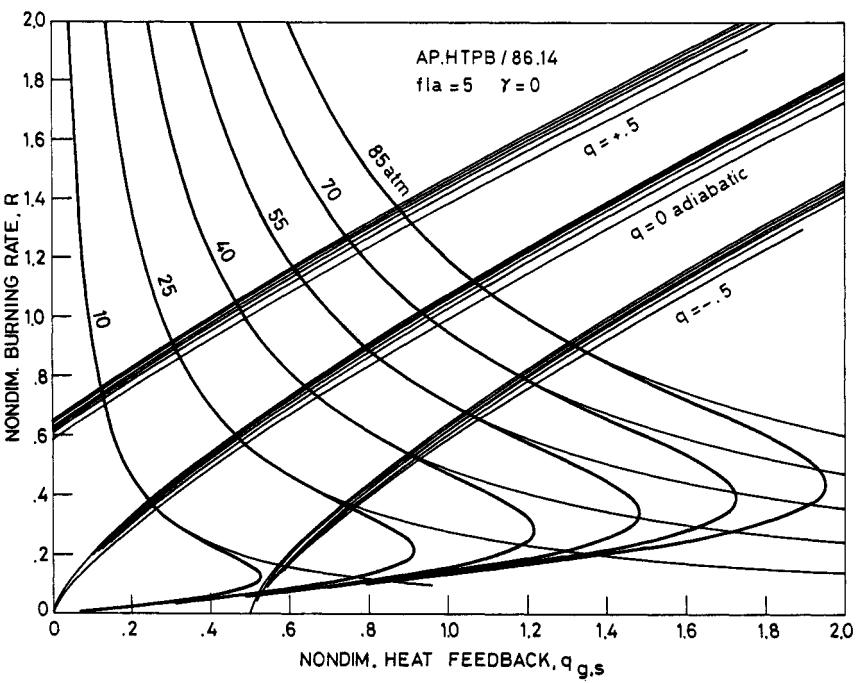

Fig. 2. Burning rate vs heat feedback according to nonlinear and linear versions of anchored flame models. For burning rates near or above steady values, the two versions do not differ.

Experimental difficulties make very difficult in general this type of data collection from composite propellants. However, few suggestions are available from different sources, usually of indirect nature (refs. 25–29), since thermal profiles are impervious to obtain. Early studies report for AP–based nonaluminized composite propellants flame thicknesses of the order of few 1000 μm (by CN emission in refs. 25–26). Recent experimental investigations conducted by Edwards et al. (refs. 27–28) showed that emission spectroscopy and Laser Induced Fluorescence (LIF) of CN radicals feature similar trends, but LIF technique enjoys much finer resolution in both space and time (see Fig. 11 of ref. 28); the observed flame thickness was respectively few 1000 μm (ref. 27) or several 100 μm (ref. 28). In any event, it is remarkable how little the few available data depend on pressure (at least in the range from subatmospheric to 8 atm; see Fig. 21 of ref. 28). Similar behavior was found for ammonium nitrate (AN)–based and HMX composite propellants. The presence of Al was found to stretch out the flame zone (p. 3501 of ref. 28 in agreement with 2–D LIF imaging results at atmospheric pressure of ref. 29).

Thermal profiles of laboratory AP–based composite propellants were systematically collected by Zenin (ref. 15). Flame thicknesses were found to decrease from few 100 μm to several 10 μm for increasing pressure from 5 to 100 atm (see Table 3 and Figs. 13–15 of ref. 15). Coarse AP particles would yield temperature fluctuations of ± 50–100 K and a prolonged tail of the temperature profile in its final end. Thermal profiles would otherwise show no appreciable differences, over the large pressure range tested and as long as AP size is less than 100 μm, by changing binders, stoichiometric ratios, and particle sizes. Other thermal profiles, scattered in several papers by Kubota and coworkers (e.g., see Figs. 4–5 of ref. 30), roughly indicate a similar behavior.

No matter how questionable the above experimental results are, the basic message is that certainly the observed flame thicknesses are much larger than currently computed by anchored or sheet transient flame models, for both DB and composite propellants.

In order to overcome at least some of the above discrepancies, a new transient flame model (conveniently called $\alpha\beta\gamma$, although different formulations are available resorting to different submodels) has been under development by the Milan group (refs. 19–24) in the recent years. The first mathematical formulation of a spatially thick transient flame model, restricted to characteristic gas–phase time depending on pressure only, was offered in ref. 19, concerning mainly transient burning and intrinsic combustion stability of DB propellants. Then, the limited validity of both spatially thin and thick transient flame models, even including temperature dependent thermodynamic properties in the condensed–phase, was recognized in ref. 20. Acknowledging a poor state of the affairs, a more general formulation of spatially thick transient flame model, allowing temperature dependence also for the gas–phase characteristic time, was offered in ref. 21, concerning mainly transient burning and intrinsic combustion stability of AP–based composite propellants. A detailed application of $\alpha\beta\gamma$ transient flame model to a catalyzed DB propellant, excluding the super–rate region, was presented in ref. 22, while an initial attempt to understand the intricacies of the super–rate region was discussed in ref. 23. All of these studies concern a propellant strand burning in an open vessel; computations of AP–based propellants burning in a confined geometry, by $\alpha\beta\gamma$ transient flame model and including pressure coupling, were reported in ref. 24. Mathematical details are given in section 5. In parallel with these efforts, this writer has been developing approximate but nonlinear approaches capable to extract the intrinsic combustion stability features concealed in transient flame models in general (refs. 19,23).

4 SURFACE HEAT RELEASE

A special side of transient flame models is the treatment of surface heat release, also for the spectacular effects on combustion dynamics and intrinsic stability of such a parameter. In refs. 3 and 10 constant values were assigned to surface heat release, by enforcing equal specific heats for the condensed– and gas–phase ($c_c = c_g$); this is very convenient but usually unrealistic. Others (refs. 4–5) enforce a temperature dependence of the surface heat release recognizing that in general $c_c \neq c_g$; this is a simple but far reaching extension. First extensive work in this specific area is mainly due to Marxmann and Wooldridge (refs. 31–33), but it was already pointed out in ref. 10 (p. 11) that their treatment of separating surface heat release in two parts (one pressure independent and the other pressure dependent) is too artificial (ref. 32). Recognizing the importance of the pressure dependent term, the same authors proposed in ref. 33 a transient flame model consisting of two delta functions respectively for the surface and gas–phase energy sources. Mongia and Ambs (ref. 34) later enforced a variable (time dependent) surface heat release, but based on questionable mathematical formalism and physical ground. Suhas and Bose (ref. 35) enforced both a constant and a variable (partially pressure dependent) surface heat release; the treatment is based on the questionable postulates of refs. 31–32. However, the importance of the dynamics of the condensed–phase heat release and its dependence on the instantaneous properties near the burning surface was correctly recognized in all of the above contributions. In the work performed by the Milan group, variable surface heat release was initially implemented by incorporating an explicit dependence on surface temperature only (see ref. 13, for example); presently, the experimentally deduced steady pressure dependence is incorporated as well (refs. 22–24).

Extensive work carried out over the years by the Milan group has shown perceivable but not essential differences between concentrated heat release at the burning surface and (volumetrically) distributed heat release in the condensed–phase. In general, most important is the intensity of the energy source rather than its space distribution. However, multi–step distributed pyrolysis has yet to be studied.

Finally, surface pyrolysis models, although not a specific ingredient of transient flame modeling, exert a relevant role on the gas–phase behavior and therefore should properly be addressed. Since an acceptable physical picture has yet to be found for the complex phenomena occurring at the burning surface, the only safe procedure is to resort to experimental information (see section 1). Yet, the question always arises as to the "best" fitting procedure of the collected experimental data. Extensive work carried out by the Milan group suggests that no conclusive evidence exists for pressure effects on the surface pyrolysis under steady operations. Since it would be puzzling to account for such effects under transient operations, pressure dependence is totally neglected in the modeling work by this research group. It follows that fitting of the experimental data is performed only through surface activation energy (possibly, different values over different ranges of surface temperature); in any event, $n_s \equiv 0$.

5 A UNIFYING MATHEMATICAL FORMALISM

Consider a strand of solid rocket propellant burning, with no velocity coupling, in a vessel at uniform pressure and possibly subjected to a radiant flux originated exclusively from a continuous external source. Assume monodimensional processes, no radiation scattering, no photochemistry, and irreversible gasification. Define a cartesian x–axis with its origin anchored at the burning surface and positive in the gas–phase direction; see sketch of Fig. 1c. Nondimensional quantities are obtained by taking as reference those (maybe nominal) values associated with the conductive thermal wave in the condensed–phase at 68 atm under adiabatic operations.

For all quasi–steady gas–phase flames of thermal nature, the nondimensional heat feedback from the gas–phase to the burning surface is

$$(3.1) \qquad q_{g,s}(P,R) = \int_{0^+}^{X_f} H_g \epsilon_g \frac{\rho_g}{\rho_c} \exp\left(-\frac{C_g}{K_g} RX\right) dX \ ,$$

where the usual assumption is made that

$$(3.2) \qquad (\partial\theta/\partial X)_{g,s} >> (\partial\theta/\partial X)_f \exp(-R^2 <\tau'_g>) \ .$$

The quantity $<\tau'_g>$ is a characteristic gas–phase time parameter conveniently defined (ref. 10) as

$$(3.3) \qquad <\tau'_g> \equiv <\tau_g> \frac{C_g}{K_g} \frac{\rho_c}{<\rho_g>} \ ,$$

where $<\tau_g>$ is the residence time in the gas–phase. Resorting to the quasi–steady mass conservation across the burning surface, one finds

$$(3.4) \qquad <\tau_g> \equiv \frac{X_f}{<U>} = \frac{X_f}{R} \frac{<\rho_g>}{\rho_c} \qquad \text{and}$$

$$(3.5) \qquad <\tau'_g> = \frac{C_g}{K_g} \frac{X_f}{R} \ .$$

The formal integration of Eq. (3.1) holds true for any integrable expression of the heat release rate distribution $H_g \epsilon_g \rho_g/\rho_c$. How can this quantity be modeled? Considering the nature of the collected temperature profiles from several laboratories (see section 3), the following law was originally proposed in ref. 19:

$$(3.6) \qquad H_g \epsilon_g \frac{\rho_g}{\rho_c} = \begin{cases} H_g M \left(\beta + \frac{1-\beta}{\alpha} \frac{X}{X_f}\right) & 0 \le X \le \alpha X_f \\ H_g M \left(\frac{1 - X/X_f}{1 - \alpha}\right)^{\gamma} & \alpha X_f \le X \le X_f \end{cases}$$

where M is the maximum value of the chemical reaction rate. By definition (see sketch in Fig. 1c):

$$0 \le \alpha(P) \le 1 \ , \qquad 0 \le \beta(P) \le 1 \ , \qquad \gamma(P) \ge 0 \ ;$$

while normalization in general requires

$$(3.7) \qquad M(\tau) = \frac{R(\tau)}{X_f(\tau)} \frac{\gamma + 1}{1 + \alpha \frac{\beta(\gamma+1) + \gamma - 1}{2}} \ .$$

Substituting into Eq. (3.1) and integrating, one finds for the transient heat feedback the following unified expression, valid for all the currently available transient flame models of thermal nature:

$$(3.8)\quad q_{g,s}(P,R) = \frac{H_g}{X_f(\tau)}\frac{K_g}{C_g}\frac{\gamma+1}{1+\alpha\,\frac{\beta(\gamma+1)+\gamma-1}{2}}\,F(\alpha,\beta,\gamma;\,R^2<\tau'_g>)$$

being

$$F(\alpha,\beta,\gamma;\,R^2<\tau'_g>) = \beta + \frac{1-\beta}{\alpha\,R^2<\tau'_g>} - \frac{(-1)^\gamma\,\gamma!}{(1-\alpha)^\gamma\,(R^2<\tau'_g>)^\gamma}\exp(-R^2<\tau'_g>) +$$

$$+\left[\sum_{i=1}^{\gamma}\frac{(-1)^i\,\gamma!}{(\gamma-i)!\,(1-\alpha)^i\,(R^2<\tau'_g>)^i} - \frac{1-\beta}{\alpha\,R^2<\tau'_g>}\right]\exp(-\alpha\,R^2<\tau'_g>)\ .$$

Notice that for $\alpha = 0$ (which necessarily implies $\beta = 1$) and $\gamma = 0$, the $\alpha\beta\gamma$ approach exactly recovers the results obtained by KTSS type of transient flame model. For $\alpha = 0$ and $\gamma > 0$, the flame thickness associated with $\alpha\beta\gamma$ approach is $\gamma + 1$ times larger than the thickness associated with KTSS type of flame. The $\alpha\beta\gamma$ approach yields a transient heat feedback law which can be written in both linear and nonlinear versions, just as in the case of KTSS type of flame. Notice in addition that for $\alpha = 1$ (which makes irrelevant the value of γ) and $\beta = 0$, the $\alpha\beta\gamma$ approach exactly recovers the results obtained with the flame sheet type of transient flame model, if proper care is taken of the unique mathematical nature of delta functions. Obviously, the results obtained by combining different contributions (e.g., a rectangular pulse with a delta function as done in MTS flame) can be recovered as well.

As to the characteristic time (or time parameter) of the gas–phase, proper allowance has in general to be made for both pressure and temperature dependences, especially for transient operations. This requires in general an appropriate submodel, which actually is the most difficult task of the whole approach. In this paper it is enough to assume in broad terms that:

$$(3.9)\quad <\tau'_g(P,R)> = f(P)\,g(R;E_g...)$$

where the function f(P), depending on pressure only, is evaluated under steady operations but in the spirit of gas–phase quasi–steadiness is assumed valid under transient conditions as well. The function g(R,E_g...) depends primarily, but not solely, on temperature (in the sense of gas–phase quasi–steadiness reference is made to the variable R, the instantaneous burning rate); it has to be specifically modeled for each class of solid propellant based on the prevailing physical mechanisms. For chemical reactions controlled by a second order kinetics or mass diffusion, one can respectively write, by generalizing a suggestion by ref. 10:

$$(3.10)\quad <\tau'_g(P,R)> = f(P)\,\Upsilon_f^2\exp[\,E_g\,(1/\Upsilon_f - 1)/2\,]$$

$$(3.11)\quad <\tau'_g(P,R)> = f(P)\,\Upsilon_f^{5/3}\,/\,\Upsilon_s^{7/4}\ .$$

The above expressions are recommended for nonaluminized AP–based composite propellants. For DB propellants, the following approximate but convenient expression was deduced from the excellent work by Zenin (refs. 14–15) and enforced in refs. 21–23:

$$(3.12)\quad <\tau'_g(P,R)> = f(P)\left[\exp\left(\frac{\tilde{E}_g}{\Re T_s}\right) + \exp\left(Z + \frac{\tilde{E}_g}{\Re T_{dz}}\right)\right]\ .$$

If only pressure dependence is accepted for the characteristic gas–phase time parameter and if the linearized heat feedback is enough to recover the steady–state burning rate (see comments in section 6 below), one necessarily finds (cf. p. 694 of ref. 13 for the case $\alpha = \gamma = 0$):

$$(3.13)\quad <\tau'_g(P,R)> = \frac{(\gamma+1)\quad H_g}{\overline{R}^2\left(\int_0^{\theta_s} C_c(\theta)\,d\theta - \overline{H}_s\right)}$$

for the common configuration of $\alpha \simeq 0$ and $\beta \simeq 1$.

Several gas–phase working maps were deduced in a range of pressure from 10 to 85 atm, by allowing specific heat and thermal conductivity of the tested propellant to be temperature or pressure dependent respectively in the condensed– and gas–phase. For typical values of the ballistic properties, the results obtained are shown in Fig. 2 (quasi–steady heat feedback) and Fig. 3 (quasi–steady flame thickness) for a transient flame whose characteristic time depends solely on pressure. The plots of Fig. 2 evidence, at each operating

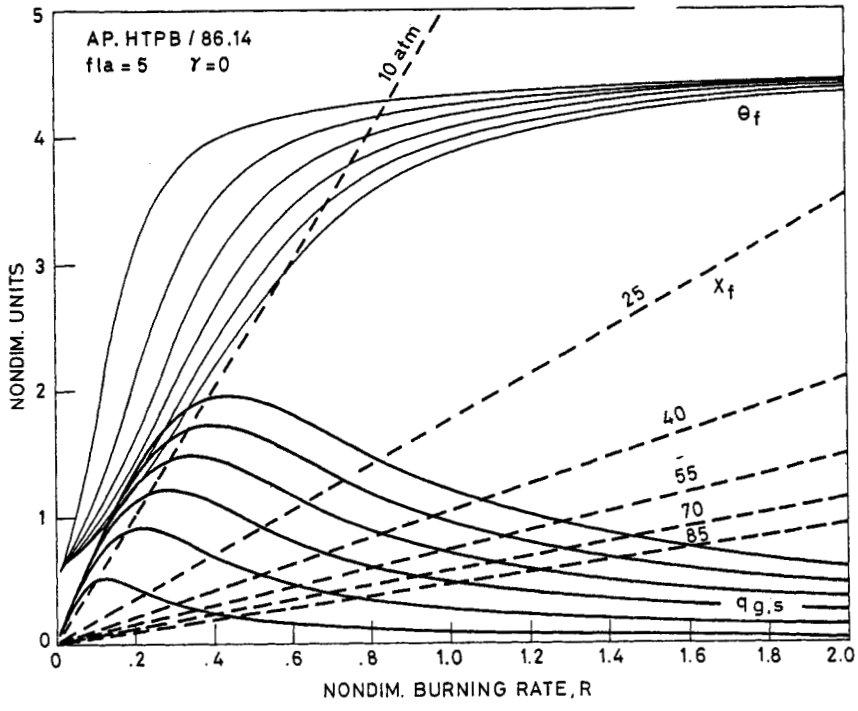

Fig. 3. Quasi-steady heat feedback, flame temperature, and flame thickness vs burning rate for anchored flame models. Identical plots are found for αβγ model for α=0, γ=0, $\langle \tau_g'(P) \rangle$. At each operating pressure, flame thickness is linear ^{g}vs burning rate.

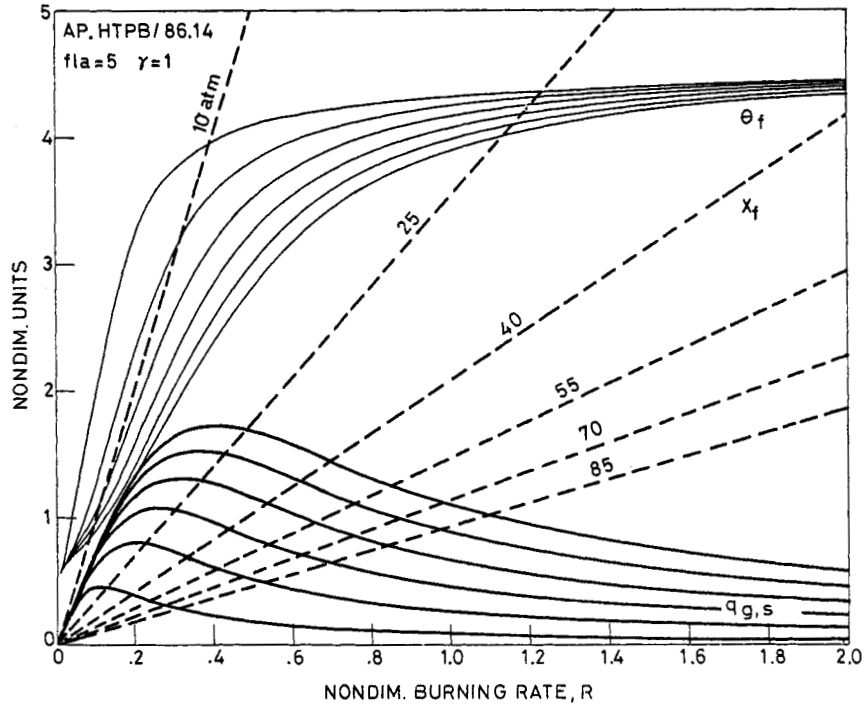

Fig. 4. Quasi-steady heat feedback, flame temperature, and flame thickness vs burning rate for αβγ model with α=0, γ=1, $\langle \tau_g'(P) \rangle$. At each operating pressure, flame thickness doubles ^{g} with respect to γ=0.

pressure, the well known behavior of heat feedback from thermal flame models; for comparison, the linearized solution ($q_{g,s} \approx 1/r_b$) is also shown. The curves crossing the figure diagonally from bottom left to top right represent the heat feedback required by the condensed–phase to sustain steady burning, at reference ambient temperature, under adiabatic (q = 0) or diabatic (q = +.5 and q = −.5) conditions; since variable properties were enforced, some pressure dependence is found for these curves as well. Therefore, two families of curves are generated describing respectively the transient heat feedback provided by the gas–phase [for example, by implementing Eq. (3.8)] and the steady heat feedback required by the condensed–phase; both are pressure dependent. Where the two families of curves overlap, for selected operating pressure and diabaticity, there the steady–state solution valid for the overall combustion wave is singled out. The effects of positive diabaticity are obvious: burning rate increases while heat feedback decreases with respect to the adiabatic case. The opposite effects are seen for negative diabaticity, but with an interesting additional result: steady–state solutions are no longer allowed if the heat loss is too large with respect to the heat feedback furnished by the gas–phase, as shown in Fig. 2 at 10 atm. Boundaries for the existence of steady state solutions can easily be constructed by plotting curves of the required condensed–phase steady heat feedback for several values of diabaticity (or ambient temperature or any other pertinent parameter). These "existence" boundaries are different from stability boundaries, which in general require much more sophisticated analyses.

The heat feedback curves of Fig. 2 are replotted in Fig. 3 vs burning rate, together with flame temperature and flame thickness; while flame temperatures tend to coalesce for large burning rates, flame thicknesses manifest a linear dependence on burning rate decreasing for increasing pressures. The results of Figs. 2–3 were collected by enforcing the $\alpha\beta\gamma$ model with $\alpha = 0$, $\beta = 1$, and $\gamma = 0$; therefore, identical plots would be found by implementing KTSS or KZ or LC models. However, the effects of a larger flame thickness can be studied only by enforcing the $\alpha\beta\gamma$ model. By just putting $\gamma = 1$, the results of Fig. 4 (to be contrasted with Fig. 3) are obtained; notice that the flame thickness doubles, while the flame temperature is not sensibly affected. This implies, in turn, a weakening of the energetic coupling at the burning surface and finally a decrease of the intrinsic combustion stability. These effects, however, are strongly tempered by the fact that the characteristic gas–phase time was considered only pressure dependent in the computations of Figs. 2–4, as tacitly but commonly assumed in literature. If, in addition, one allows temperature dependence for the gas–phase characteristic time, for example through a diffusion mechanism, then the results of Fig. 5 are collected. The weakening of the energetic coupling of such a flame with the condensed–phase is more evident, leading ultimately to a further decrease of the intrinsic combustion stability. Notice that, under these operating conditions, the dependence of the flame thickness vs burning rate is no longer linear, in particular in the range of low burning rates. This trend is further emphasized if temperature dependence through a kinetic mechanism is enforced; again, the flame thickness would no longer be found linear vs burning rate.

For a matter of space, only the summarizing picture of Fig. 6 is given, where the characteristic gas–phase time parameter is plotted vs burning rate for the different submodels just discussed. The opposite trends between diffusion and kinetics controlled mechanisms, in the low burning rate region, is dramatic; on the other hand, the behavior of the submodel with only pressure dependent characteristic gas–phase time is trivial. An attempt to combine diffusive and kinetics effects, in the spirit of MTS flame but without its limitations, is also shown in Fig. 6; obviously, the results are strongly dependent on the way that the two effects are combined. The main message from the above results is that basic knowledge is badly missing in this area. Moreover, fundamental mechanisms are tightly related to the specific nature of the burning propellant. Approaches based on artificial mechanisms may be very deceiving. It is underlined that combustion dynamics and intrinsic stability heavily depend on the details of the implemented kinetic scheme; in comparison, any other factor vanishes.

Finally, the overall approach for transient modeling of spacewise thick flames consists of the following. First, $X_f(\tilde{P})$ is experimentally measured under steady operations; from this, $\gamma(P)$ is evaluated by a best fitting procedure and $<\tau'_g(\tilde{P})>$ is computed through Eq.(3.5) [or, equivalently, $<\tau_g(\tilde{P})>$ is computed through Eq.(3.4)]. Then, under nonsteady operations, the instantaneous $<\tau'_g(P,R)>$ [or, equivalently, $<\tau_g(P,R)>$] is computed through a proper submodel by just introducing the instantaneous values of the relevant quantities. The transient flame thickness $X_f(\tau)$ at this stage is computed backward through Eq. (3.5) [or Eq. (3.4)]. It is obvious that the simple mass balance across the burning surface, in terms of either Eq. (3.5) or Eq. (3.4), is the pivotal point for the whole procedure.

6 NONLINEAR COMBUSTION STABILITY

Analysis of (intrinsic) combustion stability requires mathematical developments out of the scope of this paper. This writer presented an approximate but nonlinear approach (ref. 13) capable to easily extract the combustion stability features intrinsically embodied in any transient flame model. A given steady combustion configuration of a burning propellant is defined as asymptotically stable if random natural disturbances disappear at large times, so that the burning propellant recovers its initial (unperturbed) steady combustion configuration. This kind of stability problems can be denoted as "static", in contrast with the "dynamic" stability problems.

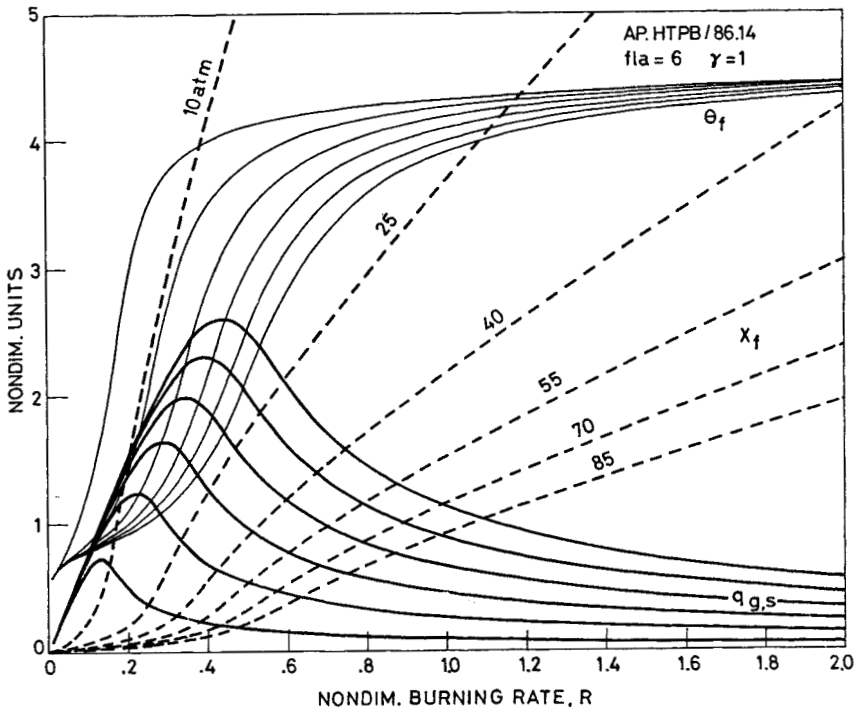

Fig. 5. Quasi-steady heat feedback, flame temperature, and flame thickness vs burning rate for αβγ model with α=0, γ=1, $\langle\tau'_g(P,R)\rangle$ diffusive. At each operating pressure, flame thickness collapses for low burning rates.

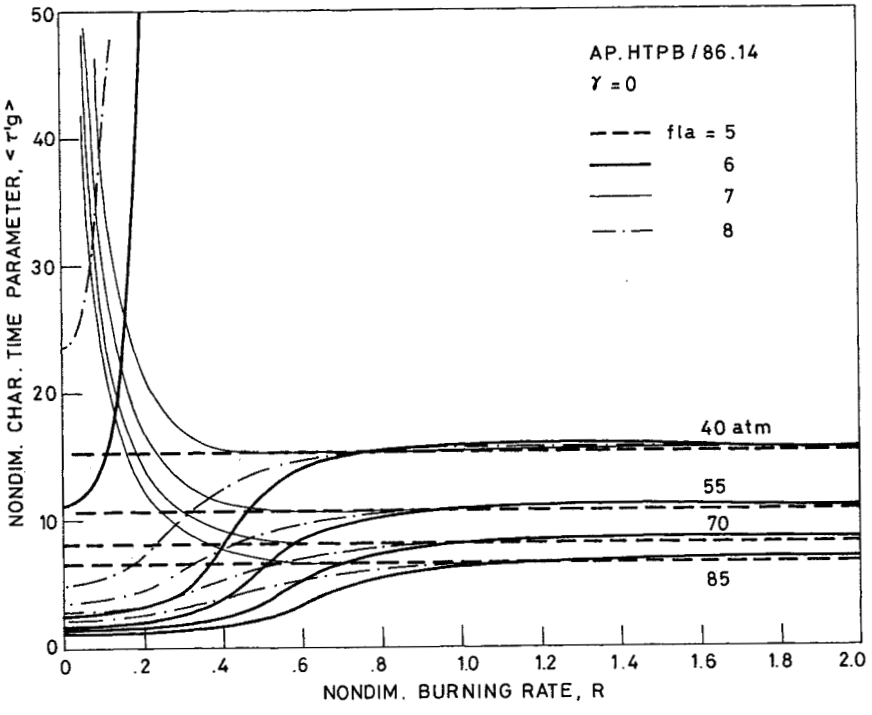

Fig. 6. The characteristic gas-phase time parameter, at each operating pressure, is virtually constant for burning rates near or above steady values, but changes dramatically for low burning rates. Flame model code: 5 is $\langle\tau'_g(P)\rangle$; 6 is $\langle\tau'_g(P,R)\rangle$ diffusive; 7 is $\langle\tau'_g(P,R)\rangle$ kinetic; 8 is $\langle\tau'_g(P,R)\rangle$ combined.

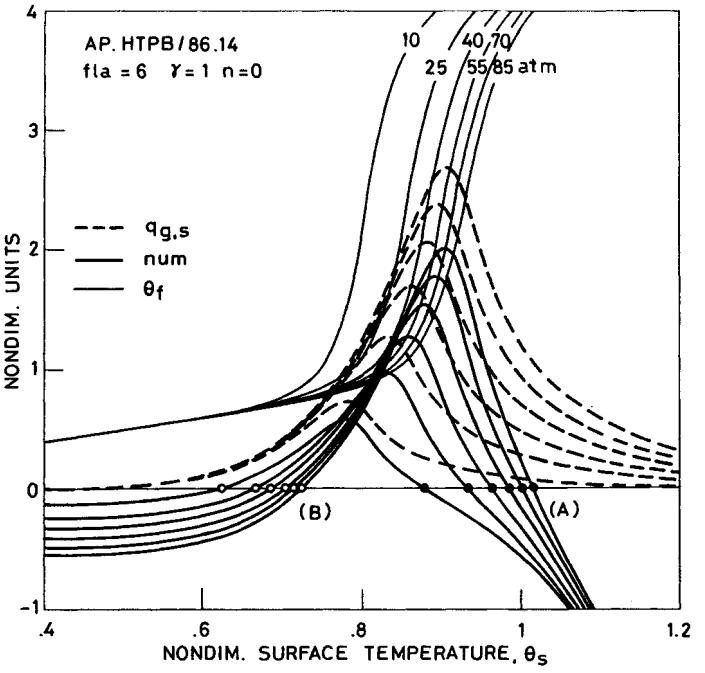

Fig. 7. Numerator of nonlinear restoring function and quasi-steady heat feedback and flame temperature vs surface temperature for αβγ model with α=0, γ=1, $<\tau_g'(P,R)>$ diffusive. At each operating pressure: steady-state solutions (roots A) correspond to fully developed flames; dynamic extinction limits (roots B) correspond to marginally developed flames.

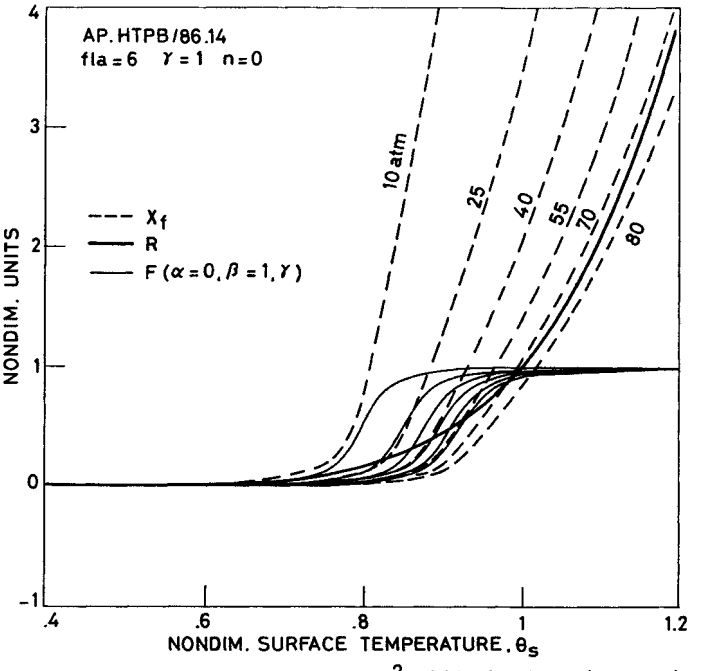

Fig. 8. Burning rate, $F(\alpha,\beta,\gamma;R^2<\tau_g'(P,R)>$ function, and quasi-steady flame thickness vs surface temperature for αβγ model with α=0, γ=1, $<\tau_g'(P,R)>$ diffusive. At each operating pressure, for low burning rates flame thickness decreases faster than the burning rate.

Static combustion stability is concerned with the stability of steady–state burning solutions, whose existence is assumed. In this respect, static stability analyses by KTSS, KZ, and LC transient flame models are equivalent in both the linearized and nonlinear versions. Likewise, MTS and the whole family of $\alpha\beta\gamma$ transient flame models manifest very close results. The reason for this broad agreement is simple: all of these transient flame models, if properly implemented, incorporate the experimentally observed steady–state burning configuration. The theoretical stability predictions are equivalent to the extent in which this is actually realized; KZ and MTS transient flame model may be less accurate in this regard. Likewise, linearized and nonlinear transient flame models are equivalent to the extent in which they are able to recover the steady–state burning configuration; in this regard differences are usually negligible, even though linearized versions may be defective in the low burning rate region, especially for low operating pressures (see Fig. 2).

Dynamic combustion stability is concerned with the stability of burning transitions, between two steady–state configurations, driven by an externally assigned change in time of a forcing function (pressure, typically); the two steady configurations are both assumed existing and statically stable. Although this nomenclature is traditionally accepted in literature, dynamic stability should rather be called "transitional". At any rate, only the nonlinear versions of transient flame models are able to describe finite size burning transitions and, therefore, possible effects of dynamic instability. Typically, in a forced depressurization and/or deradiation, extinction will occur if the driving disturbance is too severe; in this special but practically relevant case, dynamic stability boundary simply means dynamic extinction boundary. It was shown (pp. 716–717 of ref. 13) that the statically unstable root of the perturbed energy equation defines that ultimate burning rate (or surface temperature), under which extinction necessarily occurs during a forced monotonic decrease of pressure and/or radiant flux. This ultimate value is a property of the burning propellant, which can be computed. The results, obtained by implementing the $\alpha\beta\gamma$ model with $\alpha = 0$, $\beta = 1$, $\gamma = 1$ and a characteristic gas–phase time depending on temperature through a diffusion mechanism, are shown in Figs. 7–8. The essential combustion stability information are contained in the plot of the function called num (the numerator of the nonlinear static restoring function discussed at length on pp. 706–711 of ref 13): roots A are the statically stable steady–state solutions, while roots B are the statically unstable solutions defining the dynamic extinction limit at each operating pressure. In the same figure, the behavior of the quasi–steady flame temperature and heat feedback is plotted vs surface temperature. It can be seen that, at each operating pressure, the steady–state solution (root A) is located in a region where the flame is fully developed, while the dynamic extinction limit (root B) is located in a region where the flame is only marginally developed. It is underlined that all roots are solutions of the perturbed energy equation; roots A exactly coincide with the corresponding experimentally observed steady–state solutions (within the restrictions above discussed if linearized models are enforced); roots B can only be deduced (experimentally or numerically) through go/no–go testing. It is also of interest the fact that, at each operating pressure, roots B are systematically found for heat feedback values less than the maximum value associated with that pressure (in turn, roughly corresponding to the existence boundary of steady–state solutions). Further details of the combustion stability analysis are illustrated in Fig. 8, where the quasi–steady flame thickness is seen to behave as the burning rate in the high burning rate region, but as the function $F(\alpha,\beta,\gamma; R^2<\tau'_g>)$ in the low burning rate region; this proves that temperature effects through the assumed diffusion mechanism are dominating in the low burning rate region.

A direct comparison of plots of the kind of Fig. 7 does not evidence dramatic differences in terms of extinction limits, although numerical simulation of burning dynamics may be strongly affected by the selection of the transient flame model. The reason for this is the fact that the resistance to burning rate changes during transient operations does not directly depend on the value of root B (which is the ultimate limit beyond which dynamic extinction occurs), but rather on the area subdued by the nonlinear static restoring function (of which the function num in Fig. 7 is a factor). It is found that among nonlinear transient flame models KTSS, KZ, LC, and $\gamma=0$ (being $\alpha=0$ and $\beta=1$) feature the strongest resistance to dynamic burning; any temperature effect added through diffusive or kinetic mechanism (including MTS model) is sensibly destabilizing; these effects are further emphasized by the simultaneous occurrence of large flame thickness in space ($\gamma>0$). For a matter of space, this argument cannot be developed in details; the interested reader might however wish to read refs. 19–21.

7 CONCLUSIONS

A review was given of the main problems facing transient flame modeling of solid rocket propellants. The question of spatially thick transient flames can easily be overcome, once appropriate experimental information is available. Spatially thick flames in general are intrinsically less stable and, therefore, more sensitive to dynamic burning conditions; the reason for this, being the weaker energetic coupling prevailing at the burning surface between condensed– and gas–phase. The most important factor, however, affecting transient flames is the temperature dependence of the gas–phase characteristic time. In spite of the initial progress made in this area, more fundamental work needs to be done with specific reference to the detailed nature of the burning solid propellant. The analysis so far accomplished points out that temperature dependence of both chemical kinetics and mass diffusion makes a flame intrinsically less stable; in addition, kinetics effects are sensibly dominant over diffusive effects. This makes DB flames much more responsive to external or intrinsic disturbances than composite propellant flames. Detailed studies of the fundamental processes occurring in the gas–phase are required to accomplish further progress, with particular reference to the chemical kinetics networks of premixed flames originated from solid rocket propellants burning under widely different and varying operating conditions.

REFERENCES

1. M. Summerfield and H. Krier, AIAA Paper No. 69–178, (1969).
2. K.K. Kuo and J.P. Gore,"Transient Burning of Solid Propellants", in : Fundamentals of Solid Propellant Combustion, edited by K.K. Kuo and M. Summerfield, AIAA Progress in Astronautics and Aeronautics, Vol. 90, 599–659 (1984).
3. H. Krier, J.S. T'ien, W.A. Sirignano, and M. Summerfield, AIAA J. 6, 2, 278–285 (1968).
4. D.E. Kooker and B.T. Zinn, "Numerical Investigations of Nonlinear Axial Instabilities in Solid Rocket Motors", BRL CR No. 141, (1974).
5. J.N. Levine and F.E.C. Culick, "Nonlinear Analysis of Solid Rocket Combustion Instability", AFRPL TR No. 74–75, (1974).
6. F.E.C. Culick, Astronautica Acta 14, 2, 171–181 (1969).
7. F.E.C. Culick and G.L. Dehority, Combustion Science and Technology 1, 193–204 (1969).
8. N.S. Cohen and L.D. Strand, AIAA J. 18, 8, 968–972 (1980).
9. Z. Jian, R.E. Hamke, and J.R. Osborn, AIAA Paper No. 89–0300, (1989).
10. C.L. Merkle, S.L. Turk, and M. Summerfield, "Extinguishment of Solid Propellants by Rapid Depressurization", Princeton University, AMS Report No. 880, (1969). See also: AIAA Paper No. 69–176, (1969)
11. J.S. T'ien, Combustion Science and Technology 5, 2, 47–54 (1972).
12. H.K. Suhas and T.K. Bose, Combustion and Flame 28, 145–153 (1977). See also: "Comments", Combustion and Flame 31, 329–332 (1978); "Comments", Combustion and Flame 35, 213–218 (1979).
13. L. De Luca, "Extinction Theories and Experiments", in : Fundamentals of Solid Propellant Combustion, edited by K.K. Kuo and M. Summerfield, AIAA Progress in Astronautics and Aeronautics, Vol. 90, 661–732 (1984).
14. A.A. Zenin, Explosion Combustion and Shock Waves 19, 4, 444–446 (1983).
15. A.A. Zenin, "Thermophysics of Stable Combustion Waves of Solid Propellants", Accepted for publication in: Nonsteady Burning and Combustion Stability of Solid Propellants, a forthcoming AIAA Progress Series volume.
16. R. Klein, M. Menster, G. Von Elbe, and B. Lewis, Journal of Physical and Colloid Chemistry 54, 877–884 (1950).
17. N. Kubota, T.J. Ohlemiller, L.H. Caveny, and M. Summerfield, " The Mechanism of Super–Rate Burning of Catalyzed Double–Base Propellants", Princeton University, AMS Report No. 1087, (1973).
18. M.S. Miller, Combustion and Flame 46, 51–73 (1982).
19. L. De Luca, C. Zanotti, G. Riva, R. Dondé, A. Volpi, C. Grimaldi, and G. Colombo, "Burning Stability of Double–Base Propellants", AGARD PEP 66th (A) Specialists' Meeting on Smokeless Propellants, Conference Proceedings No. 391, paper 10, (1986).
20. C. Bruno, R. Dondé, G. Riva, and L. De Luca, "Computed Nonlinear Transient Burning of Solid Propellants with Variable Thermal Properties", 17th International ICT Conference, Proceedings, paper 73, (1986).
21. L. De Luca, G. Riva, C. Bruno, C. Zanotti, R. Dondé, C. Grimaldi, and G. Colombo, "Modeling of Spacewise Thick Flames", XXXVI International Astronautical Federation Congress, IAF Paper No. 86–196 (1986).
22. L. De Luca, L. Galfetti, G. Colombo, C. Grimaldi, C. Zanotti, and M. Liperi, "Transient Modeling of Spacewise Thick Flames for Rocket Propulsion", Symposium on Commercial Opportunities in Space, Taiwan, China, (1987).
23. C. Grimaldi, G. Colombo, L. Galfetti, F. Turrini, C. Zanotti, and L. De Luca, "Modeling of Catalyzed Double–Base Transient Flames", IX Congresso Nazionale AIDAA, Palermo, Italy, (1987).
24. L. Galfetti, F. Turrini, and L. De Luca, "Modeling of Transient Combustion in Solid Rocket Motors", XVI International Symposium on Space Technology and Science, Proceedings, 217–227 (1988).
25. L.A. Povinelli, AIAA J. 3, 9, 1593–1598 (1965).
26. R. L. Derr, "An Experimental Investigation of the Gaseous Phase Reaction Zone in a Composite Solid Propellant", Ph. D. Thesis, Department of Mechanical Engineering, Purdue University (1967).
27. T. Edwards, D.P. Weaver, D.H. Campbell, and S. Hulsizer, J. Propulsion 2, 3, 228–234 (1986).
28. T. Edwards, D.P. Weaver, and D.H. Campbell, Applied Optics 26, 17, 3496–3509 (1987).
29. T.P. Parr and D. Hanson–Parr, "Species and Temperature Profiles in Ignition and Deflagration of HMX", Western States Section/Combustion Institute Paper WSS/CI No. 87–8 (1987).
30. T. Kuwahara and N. Kubota, J. Spacecrafts and Rockets 21, 5, 502–507 (1984).
31. G.A. Marxman and C.E. Wooldridge, AIAA J. 6, 3, pp. 471–478 (1968).
32. C.E. Wooldridge and G.A. Marxman, AIAA Paper No. 69–172, (1969).
33. C.E. Wooldridge and G.A. Marxman, AIAA Paper No. 70–666, (1970).
34. H.C. Mongia and L.L. Ambs, Combustion and Flame 22, 59–69 (1974). See also: "Comments", Combustion and Flame 23, 401–402 (1974).
35. H.K. Suhas and T.K. Bose, Combustion Science and Technology 28, 55–68 (1982).